Int. J. Solids Structures Vol. 30, No. 9, pp. 1255–1268, 1993
Printed in Great Britain

0020–7683/93 $6.00+ .00
Pergamon Press Ltd

NONLINEAR VIBRATIONS OF HEATED ANTI-SYMMETRIC ANGLE-PLY LAMINATED PLATES

A. BHIMARADDI†
Diversified Computer Engineering and Development, 11 West 14 Mile Road, Suite 205, Clawson, MI 48017, U.S.A.

and

K. CHANDRASHEKHARA
Department of Mechanical and Aerospace Engineering and Engineering Mechanics, University of Missouri-Rolla, Rolla, MO 65401-0249, U.S.A.

(*Received* 18 *July* 1991; *in revised form* 10 *October* 1992)

Abstract—Large amplitude vibrations, buckling and post-buckling analysis of heated angle-ply laminated plates have been considered using the parabolic shear deformation theory. Strains due to initial imperfections have also been retained using the von Karman type large deflection model. Numerical results are obtained by using the single mode approach to simply-supported plates, thus reducing five governing equations to a single nonlinear time differential equation involving quadratic and cubic nonlinearities. The effects of initial imperfections and the temperature loading on the response characteristics of the plate have been studied. Numerical results for isotropic and anti-symmetric angle-ply plates have been presented and discussed.

INTRODUCTION

It is well known that composite materials have a definite advantage over metallic materials in that they can be tailor-made to suit the load environment. However, due to their anisotropic nature, analysis of such structures poses considerable mathematical problems as compared to metallic material structures. Laminated plates made of composite materials are the basic structural elements in many modern day industries, such as the aerospace and automobile industries. It is needless to say that these structures are subjected to a variety of loadings, including thermal loads. Thus, thermally induced deformation analysis of laminated plates becomes an important consideration while designing.

Thermal buckling of laminated plates is considered to be a potential failure mechanism in many structures. It may be seen from the available literature [see for example, Leissa (1981)] that there is a lot written about the buckling of plates subjected to mechanical loads as compared to that subjected to thermal loads. Buckling of laminated plates under thermal loads is of recent origin. Stavsky (1963, 1975), Biswas (1976), Bargmann (1985), Tauchert (1987), and Chen and Chen (1987) have considered the thermal buckling of plates using analytical methods. Static stress and deformation analysis of plates subjected to thermal loads has been given by Wu and Tauchert (1980) and Tauchert (1986). An excellent account of the current knowledge on the static thermal problems of laminated plates may also be found in the above article by Tauchert (1986).

It may be mentioned here that, as compared to the static analysis of plates, there is not much work done on the nonlinear dynamic response of plates in thermal environments. Pal (1973) presented the nonlinear static and dynamic analysis of heated orthotropic circular plates. Huang and Tauchert (1988) have studied large deflection static analysis of plates subjected to nonuniform thermal loading. Linear transient response of plates subjected to thermal shock has been considered by Tauchert (1989).

Excepting the works of Tauchert (1986, 1987), Chandrashekhara (1990), Chang (1990), and a few others, it is clear from the above mentioned works that the thermal response of plates has mostly been studied by using the classical Kirchhoff–Love plate theory equations.

† Current address: Ford Motor Company, Suite 800, Village Plaza, 23400 Michigan Avenue, Dearborn, MI 48124, U.S.A.

Because the shear deformation effects play a major role in the accurate determination of the response characteristics of laminated plates, it is appropriate to use some kind of shear deformable plate theory to analyse the same. Chandrashekhara (1990), Thangaratnam *et al.* (1989), and Chang (1990) have studied thermal buckling of laminated plates using the finite element method, and hence, have treated more general buckling problems than one can treat using the analytical methods. The other aspect that has not been covered adequately in the literature is the influence of initial imperfections on the buckling and nonlinear response of plates under temperature loadings.

In this paper, the nonlinear response of heated, symmetric, and antisymmetric angle-ply laminated plates has been considered using the parabolic shear deformation theory of Bhimaraddi and Stevens (1984) and Bhimaraddi (1987).

Using the assumed single mode solution for the lateral deflection, five equations of motion of the problem have been reduced to a single equation governing the nonlinear dynamic response of the plate. Initial imperfections have also been considered in the present analysis in order to study their influence on the buckling and post-buckling response of plates subjected to temperature loading. A brief description of the basic equations of the parabolic shear deformation theory (PSD) will be presented next.

EQUATIONS OF MOTION OF THE PARABOLIC SHEAR DEFORMATION THEORY

Following Bhimaraddi and Stevens (1984), the displacement components are assumed to be

$$\hat{u} = u + \xi\phi - zw'; \quad \hat{v} = v + \xi\psi - zw^{\circ}; \quad \hat{w} = w, \tag{1}$$

where

$$\xi = z\left(1 - \frac{4z^2}{3h^2}\right) \quad \text{and} \quad \xi^* = \frac{\mathrm{d}\xi}{\mathrm{d}z} = \left(1 - \frac{4z^2}{h^2}\right). \tag{2}$$

In eqns (1), $\hat{u}$, $\hat{v}$ and $\hat{w}$ are the displacement of any point (x, y, z) of the plate in the x-, y- and z-directions, respectively; u, v and w are the displacements of any point on the middle surface ($z = 0$) of the plate in the x-, y- and z-directions, respectively; ϕ and ψ are the shear rotations of any point on the middle surface of the plate in addition to the flexural rotations w' and w°; $(\,)'$ and $(\,)^{\circ}$ indicate differentiation with respect to x and y, respectively; h is the total thickness of the plate (and h_1, h_2, etc. are the thicknesses of the individual plies in the case of a laminated plate). It may be seen that u, v, w, ϕ and ψ are functions of (x, y) only, and hence, the z-dependency of the displacement field has been eliminated by an *ad hoc* assumption given in eqns (1).

Using the above displacement forms and incorporating the effects of initial imperfections in the von Karman type large deflection model, the strain–displacement relations relevant to the current study are written as [see Bhimaraddi (1989)]

$$\begin{aligned}
\varepsilon_{xx} &= u' + \xi\phi' - zw'' + \tfrac{1}{2}w'^2 + w'w'_0, \\
\varepsilon_{yy} &= v^{\circ} + \xi\psi^{\circ} - zw^{\circ\circ} + \tfrac{1}{2}w^{\circ 2} + w^{\circ}w^{\circ}_0, \\
\gamma_{xy} &= u^{\circ} + v' + \xi(\phi^{\circ} + \psi') - 2zw'^{\circ} + w'w^{\circ} + w'w^{\circ}_0 + w^{\circ}w'_0, \\
\gamma_{xz} &= \xi^*\phi; \quad \gamma_{yz} = \xi^*\psi.
\end{aligned} \tag{3}$$

Using Hamilton's principle, the following equations of motion in terms of stress-resultants can be obtained [see Bhimaraddi (1989)]:

$$N'_{xx} + N^{\circ}_{xy} = (N^{\mathrm{T}}_{xx})' + (N^{\mathrm{T}}_{xy})^{\circ} + P_1\ddot{u} + P_3\ddot{\phi} - P_2\ddot{w}', \tag{4a}$$

$$N'_{xy} + N^{\circ}_{yy} = (N^{\mathrm{T}}_{xy})' + (N^{\mathrm{T}}_{yy})^{\circ} + P_1\ddot{v} + P_3\ddot{\psi} - P_2\ddot{w}^{\circ}, \tag{4b}$$

$$\bar{M}'_{xx} + \bar{M}^{\circ}_{xy} - \bar{Q}_{xx} = (\bar{M}^{\mathrm{T}}_{xx})' + (\bar{M}^{\mathrm{T}}_{xy})^{\circ} + P_3\ddot{u} + P_6\ddot{\phi} - P_5\ddot{w}', \tag{4c}$$

$$\bar{M}'_{xy}+\bar{M}^{\circ}_{yy}-\bar{Q}_{yy}=(\bar{M}^{T}_{xy})'+(\bar{M}^{T}_{yy})^{\circ}+P_3\ddot{v}+P_6\ddot{\psi}-P_5\ddot{w}^{\circ}, \tag{4d}$$

$$\begin{aligned}M''_{xx}+2M'^{\circ}_{xy}+M^{\circ\circ}_{yy}&=q+P_1\ddot{w}-P_4(\ddot{w}''+\ddot{w}^{\circ\circ})+P_2(\ddot{u}'+\ddot{v}^{\circ})+P_5(\ddot{\phi}'-\ddot{\psi}^{\circ})\\&\quad+[(N_{xx}-N^{T}_{xx})(w'+w'_0)+(N_{xy}-N^{T}_{xy})(w^{\circ}+w^{\circ}_0)]'\\&\quad+[(N_{xy}-N^{T}_{xy})(w'+w'_0)+(N_{yy}-N^{T}_{yy})(w^{\circ}+w^{\circ}_0)]^{\circ}\\&\quad+(M^{T}_{xx})''+2(M^{T}_{xy})'^{\circ}+(M^{T}_{yy})^{\circ\circ}.\end{aligned} \tag{4e}$$

q in the last equation of (4) is the applied lateral load on the plate surface, and superposed dots indicate differentiation with respect to time (t). It may be noticed here that the inertia terms (P_1, P_2, etc.) have opposite signs, when compared with the earlier work of Bhimaraddi (1987). This is so because in the earlier paper of Bhimaraddi (1987) the signs for inertia terms were assigned to make sure that the mass matrix had positive diagonal terms. Definitions for various stress-resultants and the associated boundary conditions are given in Appendix A. Equations of motion in terms of displacement parameters (u, v, w, ϕ and ψ) can be written by using eqns (3), (A1) and (A2) in eqns (4) as follows:

$$\begin{aligned}&A_{11}u''+A_{66}u^{\circ\circ}+(A_{12}+A_{66})v'^{\circ}+2\bar{B}_{16}\phi'^{\circ}+\bar{B}_{16}\psi''+\bar{B}_{26}\psi^{\circ\circ}\\&\quad=3B_{16}w''^{\circ}+B_{26}w^{\circ\circ\circ}-A_{11}(\tfrac{1}{2}w'^{2}+w'w'_0)'-A_{12}(\tfrac{1}{2}w^{\circ 2}+w^{\circ}w^{\circ}_0)'\\&\qquad-A_{66}(w'w^{\circ}+w'w^{\circ}_0+w^{\circ}w'_0)^{\circ}+(N^{T}_{xx})'+(N^{T}_{xy})^{\circ}+P_1\ddot{u}+P_3\ddot{\phi}-P_2\ddot{w}',\end{aligned} \tag{5a}$$

$$\begin{aligned}&A_{66}v''+A_{22}v^{\circ\circ}+(A_{12}+A_{66})u'^{\circ}+2\bar{B}_{26}\psi'^{\circ}+\bar{B}_{16}\phi''+\bar{B}_{26}\phi^{\circ\circ}\\&\quad=3B_{26}w'^{\circ\circ}+B_{16}w'''-A_{12}(\tfrac{1}{2}w'^{2}+w'w'_0)^{\circ}-A_{22}(\tfrac{1}{2}w^{\circ 2}+w^{\circ}w^{\circ}_0)^{\circ}\\&\qquad-A_{66}(w'w^{\circ}+w'w^{\circ}_0+w^{\circ}w'_0)'+(N^{T}_{xy})'+(N^{T}_{yy})^{\circ}+P_1\ddot{v}+P_3\ddot{\psi}-P_2\ddot{w}^{\circ},\end{aligned} \tag{5b}$$

$$\begin{aligned}&2\bar{B}_{16}u'^{\circ}+\bar{B}_{16}v''+\bar{B}_{26}v^{\circ\circ}+\bar{\bar{D}}_{11}\phi''+\bar{\bar{D}}_{66}\phi^{\circ\circ}-\bar{A}_{44}\phi+(\bar{\bar{D}}_{12}+\bar{\bar{D}}_{66})\psi'^{\circ}\\&\quad=\bar{D}_{11}w'''+(\bar{D}_{12}+2\bar{D}_{66})w'^{\circ\circ}-\bar{B}_{16}(\tfrac{1}{2}w'^{2}+w'w'_0)^{\circ}-\bar{B}_{26}(\tfrac{1}{2}w^{\circ 2}+w^{\circ}w^{\circ}_0)^{\circ}\\&\qquad-\bar{B}_{16}(w'w^{\circ}+w'w^{\circ}_0+w^{\circ}w'_0)'+(\bar{M}^{T}_{xx})'+(\bar{M}^{T}_{xy})^{\circ}+P_3\ddot{u}+P_6\ddot{\phi}-P_5\ddot{w}',\end{aligned} \tag{5c}$$

$$\begin{aligned}&2\bar{B}_{26}v'^{\circ}+\bar{B}_{16}u''+\bar{B}_{26}u^{\circ\circ}+\bar{\bar{D}}_{66}\psi''+\bar{\bar{D}}_{22}\psi^{\circ\circ}-\bar{A}_{55}\psi+(\bar{\bar{D}}_{12}+\bar{\bar{D}}_{66})\phi'^{\circ}\\&\quad=\bar{D}_{22}w^{\circ\circ\circ}+(\bar{D}_{12}+2\bar{D}_{66})w''^{\circ}-\bar{B}_{16}(\tfrac{1}{2}w'^{2}+w'w'_0)'-\bar{B}_{26}(\tfrac{1}{2}w^{\circ 2}+w^{\circ}w^{\circ}_0)'\\&\qquad-\bar{B}_{26}(w'w^{\circ}+w'w^{\circ}_0+w^{\circ}w'_0)^{\circ}+(\bar{M}^{T}_{xy})'+(\bar{M}^{T}_{yy})^{\circ}+P_3\ddot{v}+P_6\ddot{\psi}-P_5\ddot{w}^{\circ},\end{aligned} \tag{5d}$$

$$\begin{aligned}&-3B_{16}u''^{\circ}-B_{26}u^{\circ\circ\circ}-B_{16}(\tfrac{1}{2}w'^{2}+w'w'_0)'^{\circ}-B_{26}(\tfrac{1}{2}w^{\circ 2}+w^{\circ}w^{\circ}_0)'^{\circ}\\&-B_{16}(w'w^{\circ}+w'w^{\circ}_0+w^{\circ}w'_0)''-3B_{26}v'^{\circ\circ}-B_{16}v'''-B_{16}(\tfrac{1}{2}w'^{2}+w'w'_0)'^{\circ}\\&-B_{26}(\tfrac{1}{2}w^{\circ 2}+w^{\circ}w^{\circ}_0)'^{\circ}-B_{26}(w'w^{\circ}+w'w^{\circ}_0+w^{\circ}w'_0)^{\circ\circ}-\bar{D}_{11}\phi'''\\&-(\bar{D}_{12}+2\bar{D}_{66})(\phi'^{\circ\circ}+\psi''^{\circ})-\bar{D}_{22}\psi^{\circ\circ\circ}+D_{11}w^{\mathrm{IV}}+2(D_{12}+2D_{66})w''^{\circ\circ}+D_{22}w^{\circ\circ\circ\circ}\\&=q+P_1\ddot{w}-P_4(\ddot{w}''+\ddot{w}^{\circ\circ})+P_2(\ddot{u}'+\ddot{v}^{\circ})+P_5(\ddot{\phi}'+\ddot{\psi}^{\circ})\\&+[(N_{xx}-N^{T}_{xx})(w'+w'_0)+(N_{xy}-N^{T}_{xy})(w^{\circ}+w^{\circ}_0)+(M^{T}_{xx})'+(M^{T}_{xy})^{\circ}]'\\&+[(N_{xy}-N^{T}_{xy})(w'+w'_0)+(N_{yy}-N^{T}_{yy})(w^{\circ}+w^{\circ}_0)+(M^{T}_{xy})+(M^{T}_{yy})^{\circ}]^{\circ}.\end{aligned} \tag{5e}$$

The corresponding equations of motion for classical plate theory (CPT) can be obtained from the above equations of motion using $\phi=\psi=0$ (or alternately $\xi=0$) and those for the Mindlin-type constant shear deformation theory (CSD) can be obtained by using $\xi=z$. In addition, the shear correction factors are to be used in the case of CSD to correct the deficiencies of constant shear distribution and non-zero shear stress values at the top and bottom surface of the plate. Also, it is to be noted here that the present CSD is not exactly the Mindlin theory, but it is similar to it as far as all the features of the Mindlin theory, such as constant shear strain distribution and non-zero values of transverse shear strain

and stress at the extreme fibres, are concerned. In what follows, the solution of the above equations of motion are sought.

SOLUTION OF EQUATIONS OF MOTION

In the present paper, a closed form solution to a simply-supported plate is sought using the assumed mode approach, similar to an earlier paper by Bhimaraddi (1989). Hence, the following solution for the lateral displacement (w) has been assumed:

$$w = hp(t)\sin Mx \sin Ny \quad \left(M = \frac{\pi}{a};\quad N = \frac{\pi}{b}\right) \tag{6}$$

and the initial imperfections of the plate are assumed to be

$$w_0 = hp_0 \sin Mx \sin Ny. \tag{7}$$

Substituting eqns (6) and (7) in eqns (5a) and (5d) and equating the like powers of the trigonometric terms one can obtain the following expressions for u, v, ϕ and ψ for antisymmetric angle-ply laminates:

$$\begin{aligned}
u &= a_1 hp \sin Mx \cos Ny + a_2 h^2(p^2+2pp_0)\sin 2Mx \\
&\quad + a_3 h^2(p^2+2pp_0)\sin 2Mx \cos 2Ny, \\
v &= b_1 hp \cos Mx \sin Ny + b_2 h^2(p^2+2pp_0)\sin 2Ny \\
&\quad + b_3 h^2(p^2+2pp_0)\cos 2Mx \sin 2Ny, \\
\phi &= c_1 hp \cos Mx \sin Ny + c_2 h^2(p^2+2pp_0)\sin 2Ny \\
&\quad + c_3 h^2(p^2+2pp_0)\cos 2Mx \sin 2Ny, \\
\psi &= d_1 hp \sin Mx \cos Ny + d_2 h^2(p^2+2pp_0)\sin 2Mx \\
&\quad + d_3 h^2(p^2+2pp_0)\sin 2Mx \cos 2Ny.
\end{aligned} \tag{8}$$

The above solutions have been obtained by neglecting the inertia terms appearing in eqns (5a)–(5d), and we have also considered a constant temperature distribution ($T = T_0$) throughout the plate (in the x-, y- and z-directions). This means that the derivatives of the temperature stress resultants are zero in eqns (5a)–(5e). Further, for antisymmetric angle-ply laminates, it has been observed that $M^T_{xx} = M^T_{yy} = N^T_{xy} = 0$; and in addition to which, $M^T_{xy} = 0$ for symmetric angle-ply laminates when the temperature distribution is constant. The expressions for $a_1, a_2, \ldots, d_3$ can be obtained by solving the simultaneous equations given in Appendix B. Having known all the displacement parameters, one can compute the stress-resultants, using eqns (3), (A1), (A2) and (8), as

$$\begin{aligned}
N_{xx} &= s_1 hp \cos Mx \cos Ny + h^2(p^2+2pp_0)(s_2 \cos 2Mx + s_3 \cos 2Ny \\
&\qquad + s_4 \cos 2Mx \cos 2Ny + s_5), \\
N_{yy} &= s_6 hp \cos Mx \cos Ny + h^2(p^2+2pp_0)(s_7 \cos 2Mx + s_8 \cos 2Ny \\
&\qquad + s_9 \cos 2Mx \cos 2Ny + s_{10}), \\
N_{xy} &= s_{11} hp \sin Mx \sin Ny + h^2(p^2+2pp_0)s_{12} \sin 2Mx \sin 2Ny, \\
M_{xx} &= s_{13} hp \sin Mx \sin Ny + h^2(p^2+2pp_0)s_{14} \sin 2Mx \sin 2Ny, \\
M_{yy} &= s_{15} hp \sin Mx \sin Ny + h^2(p^2+2pp_0)s_{16} \sin 2Mx \sin 2Ny, \\
M_{xy} &= s_{17} hp \cos Mx \cos Ny + h^2(p^2+2pp_0)(s_{18} \cos 2Mx + s_{19} \cos 2Ny \\
&\qquad + s_{20} \cos 2Mx \cos 2Ny + s_{21}).
\end{aligned} \tag{9}$$

Expressions similar to M_{xx}, M_{yy} and M_{xy} can also be written for $\bar{M}_{xx}$, $\bar{M}_{yy}$ and $\bar{M}_{xy}$, but they are not included here for the sake of brevity, and the expressions for s_1–s_{21} are given in Appendix B. From eqns (6), (8) and (9), it may be seen that the simply-supported boundary conditions ($w = M_{xx} = u = N_{xy} = \bar{M}_{xx} = \psi = 0$) along the lines $x = 0, a$ and ($w = M_{yy} = v = N_{xy} = \bar{M}_{yy} = \phi = 0$) along the lines $y = 0, b$ are satisfied automatically. Substituting eqns (6), (7), (8) and (9) in eqn (5e) and applying the Galerkin technique, one can obtain the following equation from which the lateral displacement (p) can be determined:

$$\ddot{p}+p+3\varepsilon p_0 p^2+\varepsilon p^3 = \mu+\kappa. \tag{10}$$

The inertia terms associated with w only were retained in eqn (5e) before applying the Galerkin technique. In eqn (10), superposed dots indicate differentiation with respect to τ, and we have the following definitions for ε, τ, μ and κ:

$$\varepsilon = \frac{h^2 s_{23}}{\left[1-\Theta+2\frac{s_{23}}{s_{22}}h^2 p_0^2\right]s_{22}}, \quad \tau = \Omega_L t, \quad \Omega_L^2 = \frac{\left[1-\Theta+2\frac{s_{23}}{s_{22}}h^2 p_0^2\right]s_{22}}{P_1+P_4 M^2+P_4 N^2},$$

$$\mu = \frac{\Theta p_0}{\left[1-\Theta+2\frac{s_{23}}{s_{22}}h^2 p_0^2\right]s_{22}}, \quad \kappa = \frac{Q}{\left[1-\Theta+2\frac{s_{23}}{s_{22}}h^2 p_0^2\right]s_{22}},$$

$$Q = \frac{\int_0^a \int_0^b q \sin Mx \sin Ny \, dx \, dy}{h\int_0^a \int_0^b \sin^2 Mx \sin^2 Ny \, dx \, dy}, \quad \Theta = T_0/T_c, \quad T_c = \frac{s_{22}}{n_{xx}^T M^2+n_{yy}^T N^2}. \tag{11}$$

In eqns (11), Ω_L is the linear frequency of the plate at any given temperature rise Θ; T_c is the critical value of the temperature at which the plate buckles; n_{xx}^T and n_{yy}^T are the values of N_{xx}^T and N_{yy}^T at unit temperature rise; and the expressions for s_{22} and s_{23} are given in Appendix B. In this paper, we have considered that the plate is subjected to temperature rise only and there are no externally applied mechanical loads on the surfaces of the plate ($\kappa = 0$).

Various plate theories such as the classical plate theory (CPT), parabolic shear deformation theory of the present paper (PSD), Mindlin-type constant shear deformation theory (CSD), and the original Mindlin shear deformation theory (MSD) have been compared in this study in the context of nonlinear vibrations of plates. It has already been explained how one can obtain the CPT and CSD from the PSD by simple substitutions. It may further be noted here that even the original Mindlin theory can be deduced from PSD by substituting $\phi = \phi_m + w'$, $\psi = \psi_m + w^\circ$, and $\xi = z$ in all the relevant equations, and by using the following equation of motion (in the lateral direction) instead of that given in eqn (4e). Here ϕ_m and ψ_m are the rotations corresponding to the MSD:

$$-\bar{Q}'_{xx}-\bar{Q}^\circ_{yy} = q+P_1\ddot{w}+[(N_{xx}-N_{xx}^T)(w'+w'_0)+(N_{xy}-N_{xy}^T)(w^\circ+w_0^\circ)]'$$
$$+[(N_{xy}-N_{xy}^T)(w'+w'_0)+(N_{yy}-N_{yy}^T)(w^\circ+w_0^\circ)]^\circ. \tag{12}$$

To check the correctness of the analytical procedure and the computer implementation of the same, critical temperatures of various problems were compared with Boley and Weiner (1960) for isotropic plates, and with Chandrashekhara (1990) and Tauchert (1987) for laminated plates; they were found to be in excellent agreement with the results quoted by these references. To check the correctness of the nonlinear part of the analysis, results

were compared with Bolotin (1964) for isotropic plates. For a square isotropic plate with immovable edges the ε value in eqn (10) as obtained by Bolotin (1964) is 1.41 and the same value was also obtained from the current study using the classical plate theory.

BUCKLING AND POST-BUCKLING RESPONSE OF PLATES AT ELEVATED TEMPERATURES

In this section we consider the static problem of eqn (10). In the absence of externally applied loads ($\kappa = 0$) and neglecting the inertia terms ($\ddot{p} = 0$), the relation between temperature (Θ) and deflection (p) can be written as

$$\Theta = \frac{p(s_{22}+2s_{23}h^2p_0^2)+3s_{23}h^2p_0p^2+s_{23}h^2p^3}{s_{22}(p+p_0)}. \tag{13}$$

It may be seen from this relation that for perfect plates one is able to find the bifurcation buckling temperature [T_c as given in eqn (11)], and the post-buckling path is quadratic in p. However, for imperfect plates there is no classical bifurcation buckling phenomenon, and one has to trace the equilibrium paths by using eqn (13) at various temperature levels.

Numerical results were obtained for different thickness, aspect ratio, and lay-ups of the plate. However, only a selected set of numerical results are presented here for the sake of brevity. Table 1 gives critical temperature values for isotropic and laminated square plates with different thickness and laminae arrangements. In the numerical results presented here Graphite/Epoxy (T300/5208) with the following properties has been used as the plate material in the case of composite laminated plates:

$$E_x = 181 \text{ GPa}, \quad E_y = 10.3 \text{ GPa}, \quad G_{xy} = G_{xz} = 7.17 \text{ GPa}, \quad G_{yz} = 6.21 \text{ GPa},$$
$$\mu_{xy} = 0.28, \quad \alpha_{xx} = 0.02 \times 10^{-6} \text{ K}^{-1}, \quad \rho = 1389.23 \text{ kg m}^{-3}.$$

Here μ_{xy} is the Poisson's ratio; E_x and E_y are the Young's moduli; G_{xy}, G_{xz} and G_{yz} are the shear moduli. In the case of an isotropic plate the Poisson's ratio has been taken to be 0.3.

Table 1. Critical temperature ($T_c\alpha_{yy} \times 10^4$) values for perfect square with various thickness values

Theory	$h/a = 0.01$	$h/a = 0.05$	$h/a = 0.075$	$h/a = 0.1$
		Isotropic plate		
PSD	1.26462	31.1936	68.9873	119.783
CSD	1.26446	31.0933	68.4981	118.313
MSD	1.26446	31.0933	68.4981	118.313
CPT	1.26533	31.6334	71.1751	126.534
		Orthotropic plate		
PSD	13.8686	327.509	687.733	1119.32
CSD	13.8607	323.183	669.021	1070.87
MSD	13.8607	323.183	669.021	1070.87
CPT	13.9027	347.567	782.025	1390.27
		2-ply (45/−45) plate		
PSD	10.6078	258.123	561.316	953.271
CSD	10.6032	255.451	548.807	917.635
MSD	10.6032	255.451	548.807	917.635
CPT	10.6199	265.498	597.370	1061.992
		4-ply (45/−45/45/−45) plate		
PSD	20.8157	489.873	1024.13	1656.72
CSD	20.8056	484.316	1000.03	1594.16
MSD	20.8056	484.316	1000.03	1594.16
CPT	20.8699	521.748	1173.93	2086.99
		6-ply (45/−45/45/−45/45/−45) plate		
PSD	22.7047	532.110	1107.22	1781.28
CSD	22.6915	524.940	1076.48	1702.58
MSD	22.6915	524.940	1076.48	1702.58
CPT	22.7681	596.202	1280.70	2776.81

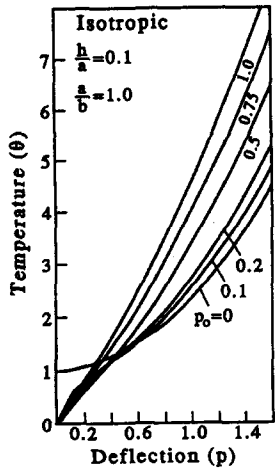

Fig. 1. Temperature vs deflection curves for imperfect isotropic plates.

It may be noted from Table 1 that the predictions of CPT differ considerably from any of the shear deformation theories for thicker plates. For example, differences of more than 25% can be seen for single, 4-ply and 6-ply plates of $h/a = 0.1$. It is interesting to note that among the shear deformation theories CSD and MSD give identical values for critical temperatures, and they are lower than those predicted by PSD. The maximum difference between MSD (or CSD) and PSD is about 4% for 6-ply plates with $h/a = 0.1$. Since CSD and MSD give identical results, only the values from CSD (or MSD) will be considered in further comparison of various theories.

Figures 1 and 2 depict post-buckling curves for perfect and imperfect plates with $h/a = 0.1$. Results obtained from PSD only are plotted in these figures since the results from CSD (or MSD) did not differ by more than 4%, and, in fact, the difference diminished as the value of plate imperfection increased. Further, differences between the post-buckling response as predicted by CPT and PSD diminished as the plate imperfection was increased. Hence, the maximum difference, as already observed in critical temperature values for perfect plates did prevail. It may be observed from these figures that the plates are imperfection insensitive, as the equilibrium paths are stable in all the cases.

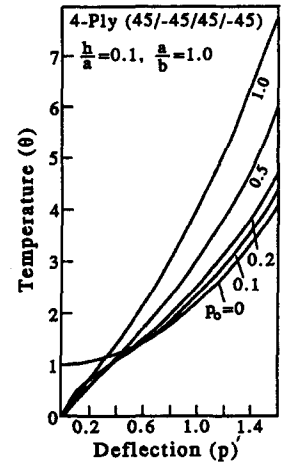

Fig. 2. Temperature vs deflection curves for imperfect 4-ply antisymmetric plates.

LARGE AMPLITUDE FREE VIBRATION OF IMPERFECT PLATES AT ELEVATED TEMPERATURES

From eqns (10) and (11) it may be seen that the consideration of an imperfect plate results in the nonlinear time differential equation that includes both the quadratic and cubic nonlinear terms. Using the method of multiple scales (Nayfeh and Mook, 1979), the following amplitude (A) dependent frequency relation can be obtained:

$$\Omega_{NL} = \Omega_L[1+3\mu\varepsilon(\tfrac{1}{2}\mu - p_0 - \tfrac{9}{2}\mu\varepsilon p_0^2) + \tfrac{3}{8}\varepsilon(1-10\varepsilon p_0^2)A^2] \tag{14}$$

and p is given by

$$p = \mu(1-3\mu\varepsilon p_0 + 18\mu^2\varepsilon^2 p_0^2 - \mu^2\varepsilon) + \varepsilon(9\mu\varepsilon p_0^2 - \tfrac{3}{2}p_0 - \tfrac{3}{2}\mu)A^2 + A\cos(t\Omega_{NL}+B)$$
$$+\tfrac{1}{2}\varepsilon(p_0 10\mu\varepsilon p_0^2+\mu)A^2\cos 2(t\Omega_{NL}+B) + \tfrac{1}{32}\varepsilon(6\varepsilon p_0^2+1)A^3\cos 3(t\Omega_{NL}+B), \tag{15}$$

where A and B are to be determined using the initial conditions. Linear frequency (Ω_{LPSD}, Ω_{LCSD} and Ω_{LCPT}) values obtained from various plate theories along with the values of ε and $3\varepsilon p_0$ [of eqn (10)] are shown in Table 2 for isotropic plates and in Table 3 for 4-ply (45/−45/45/−45) plates with different imperfection (keeping $\Theta = 0$) and temperature (keeping $p_0 = 0$) values.

In general, it may be seen from these tables that frequency increases with increasing values of p_0 and decreases with increasing values of Θ, as it should be if one observes the frequency expression in eqns (11). Comparing the frequency values predicted by various theories, it may be observed from these tables that as the temperature level increases, the difference between the various theories also increases. For example, for $\Theta = 0$ the difference

Table 2. Values of linear frequency (Ω_{LPSD}, Ω_{LCSD}, Ω_{LCPT})† and the coefficients of the nonlinear terms (ε and $3\varepsilon p_0$) for various temperatures (Θ and $p_0 = 0$) and imperfections (p_0 and $\Theta = 0$) of square isotropic plates

	Ω_{LPSD}	Ω_{LCSD}	Ω_{LCPT}	$3\varepsilon p_0$	ε
$p_0 = 0$	5.49908	5.46526	5.65192	0.0	1.390433733
= 1/10	5.57502	5.54166	5.72583	0.405844224	1.352813573
= 1/3	6.29155	6.26201	6.42557	1.062222561	1.062222561
= 1/2	7.15984	7.13389	7.27788	1.230314918	0.820209945
= 1.0	10.6927	10.6753	10.7721	1.103265649	0.367755216
$\Theta = 0$	5.49908	5.46526	5.65192	0.0	1.390433733
= 1/4	4.76235	4.72324	4.93804	0.0	1.853911644
= 1/2	3.88844	3.84045	4.10174	0.0	2.780867466
= 3/4	2.74954	2.68125	3.04373	0.0	5.561734932

† Nondimensional using $\Omega_0^2 = \dfrac{h^2}{a^4}\dfrac{E_y}{\rho(1-\mu_{xy}\mu_{yx})}$.

Table 3. Values of linear frequency (Ω_{LPSD}, Ω_{LCSD}, Ω_{LCPT})† and the coefficients of the nonlinear terms (ε and $3\varepsilon p_0$) for various temperatures (Θ and $p_0 = 0$) and imperfections (p_0 and $\Theta = 0$) of 4-ply (45/−45/45/−45) plate

	Ω_{LPSD}	Ω_{LCSD}	Ω_{LCPT}	$3\varepsilon p_0$	ε
$p_0 = 0$	14.4382	14.1629	16.2050	0.0	1.238145630
= 1/10	14.6158	14.3440	16.3635	0.362467927	1.208226425
= 1/3	16.3039	16.0604	17.8879	0.970985349	0.970985349
= 1/2	18.3715	18.1554	19.7914	1.147087659	0.764725106
= 1.0	26.9197	26.7713	27.9105	1.068505661	0.356168554
$\Theta = 0$	14.4382	14.1629	16.2050	0.0	1.238145630
= 1/4	12.5038	12.1850	14.5081	0.0	1.650860840
= 1/2	10.2093	9.81623	12.5845	0.0	2.476291260
= 3/4	7.21909	6.65156	10.30801	0.0	4.952582516

† Nondimensional using $\Omega_0^2 = \dfrac{h^2}{a^4}\dfrac{E_y}{\rho(1-\mu_{xy}\mu_{yx})}$.

between CSD and PSD is about 1.9% (Table 3), whereas for $\Theta = 0.75$ it is about 7.9%. Such differences for CPT are 12% and 43% when compared with PSD. However, it has been observed that for a given temperature level (as in Tables 2 and 3) the difference between various theories decreases as the imperfection value of the plate increases. For example, referring to Table 3, at $\Theta = 0$ the difference between CPT and PSD is about 12% for $p_0 = 0$, whereas it is only about 4% for $p_0 = 1.0$.

Further, one may observe from Tables 2 and 3 that the value of ε decreases with increasing value of imperfection, and obviously, the value of $3\varepsilon p_0$ increases as p_0 increases. It is evident from these tables that, in general, ε and $3\varepsilon p_0$ can assume values far greater than unity, as may be seen for greater temperature levels. This means that the present nonlinear plate equation (10) is one of strongly nonlinear type.

The basic assumption in obtaining the nonlinear frequency relation (14) is that the values of ε and $3\varepsilon p_0$ are less than unity. In view of this, for strongly nonlinear problems eqn (14) may not predict correct frequency values. To overcome this difficulty, the exact value of frequency can be obtained, irrespective of whether eqn (10) is strongly nonlinear or not, by using the procedure outlined in Chapter 2 of Nayfeh and Mook (1979) and also by Singh *et al.* (1991). A brief description of this procedure is given in what follows next. The total energy of the system corresponding to eqn (10) can be written as

$$H_{NL} = \tfrac{1}{2}\dot{p}^2 + \tfrac{1}{2}p^2 + \varepsilon p_0 p^3 + \tfrac{1}{4}\varepsilon p^4 - \mu p. \tag{16}$$

Since eqn (10) has quadratic and cubic nonlinearities the maximum amplitude values in the positive half of the cycle (A) and in the negative half of the cycle (A_r^*) are not equal [for details see Singh *et al.* (1991)]. At these maximum amplitude values, velocity of motion becomes zero and since the total energy of the system is constant, one can write the following:

$$H_L = -\mu A + \tfrac{1}{2}A^2 \quad \text{and} \quad H_{NL} = -\mu A + \tfrac{1}{2}A^2 + \varepsilon p_0 A^3 + \tfrac{1}{4}\varepsilon A^4. \tag{17}$$

In the above H_L is the energy of the corresponding linear system. Equating (16) and the last of eqn (17) one can obtain the following equation for velocity:

$$\dot{p}^2 = -2\mu(A-p) + (A^2 - p^2) + 2\varepsilon p_0(A^3 - p^3) + \tfrac{1}{2}\varepsilon(A^4 - p^4). \tag{18}$$

One can obtain the two maximum amplitude values by solving for the two roots of the homogeneous part of eqn (18). It is obvious from eqn (18) that one extremum amplitude (at which velocity is zero) is equal to A and let this be assumed to be of the positive side. The maximum amplitude value in the negative side (A_r^*) can be obtained as a real root (A^*) of the following equation, which can be obtained by reducing the order of the homogeneous equation (18) for a known root A:

$$2(A + 3\varepsilon p_0 A^2 + \varepsilon A^3 - \mu) - (1 + 6\varepsilon p_0 A + 3\varepsilon A^2)A^* + 2(p_0 + A)\varepsilon A^{*2} - \tfrac{1}{2}\varepsilon A^{*3} = 0. \tag{19}$$

Integrating eqn (18) one can write the nonlinear to linear frequency ratio as

$$\frac{\Omega_{NL}}{\Omega_L} = \frac{\displaystyle\int_0^A \frac{dp}{\sqrt{2H_L + 2\mu p - p^2}} + \int_0^{2\mu - A} \frac{dp}{\sqrt{2H_L + 2\mu p - p^2}}}{\displaystyle\int_0^A \frac{dp}{\sqrt{2H_{NL} + 2\mu p - p^2 - 2\varepsilon p_0 p^3 - \frac{1}{2}\varepsilon p^4}} + \int_0^{A - A_r^*} \frac{dp}{\sqrt{2H_{NL} + 2\mu p - p^2 - 2\varepsilon p_0 p^3 - \frac{1}{2}\varepsilon p^4}}}. \tag{20}$$

In general, integration in eqn (20) cannot be evaluated exactly; however, one can use numerical integration techniques to obtain the value of the frequency ratio. In this work, the Wedle's seven point integration method has been used. Nonlinear to linear frequency

Table 4. Nonlinear to linear (Ω_{NL}/Ω_L) frequency ratios for different amplitude (A) values obtained by using eqns (17) and (19) for square plates ($h/a = 0.1$, $\theta = 0$, PSD results)

	$p_0 = 1/10$		$p_0 = 1/3$		$p_0 = 1/2$	
A	eqn (17)	eqn (19)	eqn (17)	eqn (19)	eqn (17)	eqn (19)
			Isotropic plate			
0.0	1.0000	1.0000	1.0000	1.0000	1.0000	1.0000
0.2	1.0176	1.0185	0.9971	0.9980	0.9871	0.9856
0.4	1.0702	1.0772	0.9885	1.0107	0.9483	0.9505
0.6	1.1579	1.1738	0.9742	1.0808	0.8837	0.9704
0.8	1.2808	1.2984	0.9541	1.2041	0.7932	1.0812
1.0	1.4387	1.4417	0.9282	1.3511	0.6769	1.2241
			4-ply (45/−45/45/−45) plate			
0.0	1.0000	1.0000	1.0000	1.0000	1.0000	1.0000
0.2	1.0159	1.0167	0.9989	0.9997	0.9895	0.9885
0.4	1.0637	1.0692	0.9954	1.0135	0.9582	0.9616
0.6	1.1434	1.1558	0.9897	1.0751	0.9059	0.9774
0.8	1.2549	1.2688	0.9816	1.1854	0.8327	1.0734
1.0	1.3983	1.4000	0.9713	1.3207	0.7385	1.2051

Table 5. Nonlinear to linear (Ω_{NL}/Ω_L)† frequency ratios for different amplitude (A) values obtained by using eqn (19) for various theories ($a/b = 1.0$, $h/a = 0.1$, $\Theta = 0$)

	$p_0 = 1/10$			$p_0 = 1/3$			$p_0 = 1/2$		
A	PSD	CSD	CPT	PSD	CSD	CPT	PSD	CSD	CPT
				Isotropic plate					
0.0	1.000	0.994	1.027	1.000	0.995	1.021	1.000	0.996	1.017
0.2	1.019	1.013	1.045	0.998	0.993	1.020	0.986	0.982	1.003
0.4	1.077	1.072	1.102	1.0107	1.006	1.034	0.951	0.946	0.972
0.6	1.174	1.169	1.197	1.0808	1.076	1.101	0.971	0.966	0.990
0.8	1.298	1.294	1.319	1.2041	1.201	1.221	1.081	1.078	1.095
1.0	1.442	1.438	1.460	1.3511	1.348	1.365	1.224	1.222	1.235
				4-ply (45/−45/45/−45) plate					
0.0	1.000	0.982	1.120	1.000	0.985	1.097	1.000	0.988	1.077
0.2	1.017	0.998	1.135	0.999	0.984	1.10	0.989	0.976	1.070
0.4	1.069	1.052	1.182	1.014	0.998	1.116	0.962	0.947	1.055
0.6	1.156	1.140	1.260	1.075	1.061	1.169	0.978	0.964	1.068
0.8	1.269	1.255	1.363	1.185	1.174	1.265	1.073	1.063	1.144
1.0	1.400	1.387	1.485	1.321	1.311	1.389	1.205	1.197	1.261

† Ω_L corresponds to the PSD value.

ratios obtained using eqns (20) and (14) are given in Table 4. It is interesting to note from this table that the frequency ratios, as predicted by the perturbation method, decrease with increasing amplitude for $p_0 \geqslant 1/3$, whereas this is not the case with the exact method.

Thus, it may be said here that the perturbation method predicts softening behavior for p_0 values $\geqslant 1/3$, whereas the exact method indicates that the plate behavior is of the hardening type, except for lower amplitudes. Further, it may be seen that for a 4-ply plate with $p_0 = 1/3$ (Table 3) both the values of ε and $3\varepsilon p_0$ are equal but less than unity. Even in such a case, the predictions of the perturbation method are in contradiction to the exact values. However, it has also been observed that both of the methods predict comparable results for lower values of imperfections ($\leqslant 1/10$) and amplitudes. In these cases, it was seen that the values of ε were slightly greater than unity, but the values of $3\varepsilon p_0$ were much smaller than ε.

Tables 5 and 6 show the frequency ratios obtained by using the exact method for various plate theories. In general, it may be noted the CSD values are lower and CPT values are higher when compared with the PSD results. This is consistent with their prediction of linear frequencies and critical temperature values. The difference in the frequency ratios predicted by various theories diminishes as the amplitude of vibration becomes larger, thus indicating that the shear deformation effects do not prevail at these amplitudes because it has been taken over by the greater predominance of the membrane action.

Table 6. Nonlinear to linear (Ω_{NL}/Ω_L)† frequency ratios for different amplitude (A) values obtained by using eqn (19) for various theories ($a/b = 1.0$, $h/a = 0.1$, $p_0 = 0$)

	$\theta = 1/4$			$\theta = 1/2$			$\theta = 3/4$		
A	PSD	CSD	CPT	PSD	CSD	CPT	PSD	CSD	CPT
				Isotropic plate					
0.0	1.000	0.922	1.037	1.000	0.988	1.055	1.000	0.975	1.107
0.2	1.027	1.019	1.063	1.041	1.029	1.094	1.080	1.057	1.180
0.4	1.105	1.097	1.138	1.153	1.143	1.201	1.287	1.267	1.372
0.6	1.222	1.215	1.252	1.318	1.309	1.360	1.569	1.553	1.640
0.8	1.368	1.362	1.395	1.517	1.509	1.554	1.893	1.880	1.953
1.0	1.535	1.529	1.559	1.739	1.732	1.772	2.242	2.230	2.293
				4-ply (45/−45/45/−45) plate					
0.0	1.000	0.975	1.160	1.000	0.962	1.233	1.000	0.921	1.428
0.2	1.025	1.000	1.181	1.036	1.000	1.262	1.071	0.998	1.479
0.4	1.094	1.071	1.242	1.138	1.104	1.347	1.259	1.197	1.621
0.6	1.200	1.179	1.337	1.287	1.257	1.476	1.518	1.466	1.831
0.8	1.333	1.314	1.458	1.470	1.444	1.639	1.818	1.775	2.088
1.0	1.486	1.469	1.600	1.675	1.652	1.826	2.142	2.105	2.377

† Ω_L corresponds to the PSD value.

Table 7. Nonlinear to linear (Ω_{NL}/Ω_L) frequency ratios for different amplitude (A) values obtained by using eqn (19) for various ply arrangements† ($a/b = 1.0$, $h/a = 0.1$, $p_0 = 1/10$)

	$\theta = 0$			$\theta = 1/4$		
A	2-ply (11.19)‡	4-ply (14.62)	6-ply (15.14)	2-ply (9.75)	4-ply (12.71)	6-ply (13.16)
0.0	1.000	1.000	1.000	1.000	1.000	1.000
0.2	1.027	1.017	1.016	1.048	1.031	1.029
0.4	1.116	1.069	1.065	1.145	1.089	1.083
0.6	1.260	1.156	1.146	1.324	1.196	1.183
0.8	1.436	1.269	1.252	1.543	1.338	1.317
1.0	1.632	1.400	1.376	1.781	1.501	1.472

† Plies are arranged alternately at ±45° (e.g. 4-ply is 45/−45/45/−45).
‡ Nondimensionalized linear frequency values are given in parentheses.

Table 7 shows frequency ratios for an imperfect plate with different lay-ups. Here an angle ply plate (with angle = 45°) has been considered with three lay-up arrangements. It may be seen from this table, as well as from Tables 5 and 6, that the frequency ratios decrease with increasing values of p_0 and increase with increasing values of Θ, indicating that the nonlinear effects are most pronounced at elevated temperatures of imperfect plates. Also, it may be seen from this table that the 2-ply arrangement produces higher frequency ratios followed by 4-ply plates. This indicates that the nonlinear effects are higher in 2-ply antisymmetric plates as compared to 4- and 6-ply plates.

CONCLUSIONS

Large amplitude vibration of imperfect angle-ply plates at elevated temperatures has been considered using the parabolic shear deformation theory. It has been shown that the other theories, such as the classical plate theory and the constant shear deformation theory due to Mindlin can be obtained from the present parabolic shear deformation theory. Numerical results showed that the classical plate theory is inadequate to obtain the linear frequency values and the critical temperatures of plates, whereas it predicts good results in the case of large amplitude vibrations. The two shear deformation theories differ increasingly while predicting the linear frequencies of heated plates with increasing temperature levels. The increasing values of the frequency ratios indicate that the nonlinear effects are more predominant in imperfect plates and for plates at elevated temperatures. Numerical results also demonstrated that the nonlinear effects are higher in 2-ply antisymmetric plates as compared to 4- and 6-ply plates.

REFERENCES

Bargmann, H. W. (1985). Thermal buckling of elastic plates. *J. Therm. Stress.* **8,** 71–98.

Bhimaraddi, A. (1987). Static and transient response of rectangular plates. *Thin-Walled Structures* **5,** 125–143.

Bhimaraddi, A. (1989). Nonlinear free vibration analysis of composite plates with initial imperfections and in-plane loading. *Int. J. Solids Structures* **25,** 33–43.

Bhimaraddi, A. and Stevens, L. K. (1984). A higher order theory for free vibration of orthotropic, homogeneous, and laminated rectangular plates. *J. Appl. Mech.* **51,** 195–198.

Biswas, P. (1976). Thermal buckling of orthotropic plates. *J. Appl. Mech.* **43,** 361–363.

Boley, B. A. and Weiner, J. H. (1960). *Theory of Thermal Stresses.* John Wiley, New York.

Bolotin, V. V. (1964). *The Dynamic Stability of Elastic Systems.* Holden-Day, San Francisco.

Chandrashekhara, K. (1990). Buckling of multilayered composite plates under uniform temperature field. In *Thermal Effects of Structures and Materials, Proceedings of the Winter Annual Meeting of ASME,* AMD-Vol. 110, pp. 29–33.

Chang, J. S. (1990). FEM analysis of buckling and thermal buckling of antisymmetric angle-ply laminates according to transverse shear and normal deformable high order displacement theory. *Comput. Struct.* **37,** 925–946.

Chen, L. W. and Chen, L. Y. (1987). Thermal buckling of laminated composite plates. *J. Therm. Stress.* **10,** 345–356.

Huang, N. N. and Tauchert, T. R. (1988). Large deformation of antisymmetric angle-ply laminates resulting from nonuniform temperature loadings. *J. Therm. Stress.* **11,** 287–297.

Leissa, A. W. (1981). Advances in vibration, buckling and postbuckling studies on composite plates. In *Composite Structures, Proc. 1st Int. Conf.,* September 1981 (Edited by I. H. Marshall), pp. 312–334. Applied Science.

Nayfeh, A. H. and Mook, D. T. (1979). *Nonlinear Oscillations.* John Wiley, New York.

Pal, M. C. (1973). Static and dynamic non-linear behaviour of heated orthotropic circular plates. *Int. J. Non-Lin. Mech.* **8,** 489–504.

Singh, G., Venkateswara Rao, G. and Iyengar, N. G. R. (1991). Large amplitude free vibration of simply supported antisymmetric cross-ply plates. *AIAA Jl* **29,** 784–790.

Stavsky, Y. (1963). Thermoelasticity of heterogeneous aeolotropic plates. *J. Engng Mech. Div., ASCE* **89,** 89–105.

Stavsky, Y. (1975). Thermoelastic stability of laminated orthotropic circular plates. *Acta Mech.* **22,** 31–51.

Tauchert, T. R. (1986). Thermal stresses in plates—statical problems. In *Thermal Stresses—I* (Edited by R. B. Hetnarski), Chap. 2, pp. 23–141. Elsevier Science Publishers B. V., Amsterdam.

Tauchert, T. R. (1987). Thermal buckling of thick antisymmetric angle-ply laminates. *J. Therm. Stress.* **10,** 113–124.

Tauchert, T. R. (1989). Thermal shock of orthotropic rectangular plates. *J. Therm. Stress.* **12,** 241–258.

Thangaratnam, K. R., Palaninathan and Ramachandran, J. (1989). Thermal buckling of composite plates. *Comput. Struct.* **32,** 1117–1124.

Wu, C. H. and Tauchert, T. R. (1980). Thermoelastic analysis of laminated plates, 2: Antisymmetric cross-ply and angle-ply laminates. *J. Therm. Stress.* **3,** 365–378.

APPENDIX A

In this appendix the stress-resultants and the associated boundary conditions pertinent to the equations of motion (4) and (5) are given. Following Bhimaraddi (1987), the definitions for stress-resultants appropriate to the current study are written as

$$\begin{bmatrix} N_{xx} & M_{xx} & \bar{M}_{xx} \\ N_{yy} & M_{yy} & \bar{M}_{yy} \\ N_{xy} & M_{xy} & \bar{M}_{xy} \end{bmatrix} = \int_{-h/2}^{h/2} \begin{bmatrix} C_{11} & C_{12} & C_{16} \\ C_{12} & C_{22} & C_{26} \\ C_{16} & C_{26} & C_{66} \end{bmatrix} \begin{bmatrix} \varepsilon_{xx} \\ \varepsilon_{yy} \\ \gamma_{xy} \end{bmatrix} (1 \quad -z \quad \xi)\, \mathrm{d}z, \tag{A1a}$$

$$\bar{Q}_{xx} = \int_{-h/2}^{h/2} \tau_{xz} \xi^* \, \mathrm{d}z, \quad \bar{Q}_{yy} = \int_{-h/2}^{h/2} \tau_{yz} \xi^* \, \mathrm{d}z. \tag{A1b}$$

In a similar fashion, one can write the stress-resultants due to temperature change as

$$\begin{bmatrix} N_{xx}^{\mathrm{T}} & M_{xx}^{\mathrm{T}} & \bar{M}_{xx}^{\mathrm{T}} \\ N_{yy}^{\mathrm{T}} & M_{yy}^{\mathrm{T}} & \bar{M}_{yy}^{\mathrm{T}} \\ N_{xy}^{\mathrm{T}} & M_{xy}^{\mathrm{T}} & \bar{M}_{xy}^{\mathrm{T}} \end{bmatrix} = \int_{-h/2}^{h/2} \begin{bmatrix} C_{11} & C_{12} & C_{16} \\ C_{12} & C_{22} & C_{26} \\ C_{16} & C_{26} & C_{66} \end{bmatrix} \begin{bmatrix} \alpha_{xx} \\ \alpha_{yy} \\ \alpha_{xy} \end{bmatrix} (1 \quad -z \quad \xi) T \, \mathrm{d}z. \tag{A1c}$$

In the above equations, $T(x, y, z)$ is the temperature change from the ambient value and α_{xx}, α_{yy} and α_{xy} are the coefficients of thermal expansion. The definition for integrated elastic stiffness and inertia terms are given as

$$(A_{ij} B_{ij} \bar{B}_{ij} D_{ij} \bar{D}_{ij} \bar{D}_{ij}) = \int_{-h/2}^{h/2} (1 z \xi z^2 z \xi \xi^2) C_{ij} \, \mathrm{d}z,$$

$$\bar{A}_{ij} = \int_{-h/2}^{h/2} C_{ij} \xi^{*2} \, \mathrm{d}z, \quad (P_1 P_2 P_3 P_4 P_5 P_6) = \int_{-h/2}^{h/2} \rho (1 z \xi z^2 z \xi \xi^2) \, \mathrm{d}z. \tag{A2}$$

Here ρ is the mass density of the plate material. The associated boundary conditions along the line x = constant require that at least one member of the following six pairs must be specified:

$$(N_{xx}-N_{xx}^{T}) \text{ or } u, \quad (N_{xy}-N_{xy}^{T}) \text{ or } v, \quad (\bar{M}_{xx}-\bar{M}_{xx}^{T}) \text{ or } \phi,$$
$$(\bar{M}_{xy}-\bar{M}_{xy}^{T}) \text{ or } \psi, \quad (M_{xx}-M_{xx}^{T}) \text{ or } w', \quad Q_{xx} \text{ or } w \tag{A3a}$$

and those along the line y = constant require that one member of the following six pairs must be specified:

$$(N_{xy}-N_{xy}^{T}) \text{ or } u, \quad (N_{yy}-N_{yy}^{T}) \text{ or } v, \quad (\bar{M}_{xy}-\bar{M}_{xy}^{T}) \text{ or } \phi,$$
$$(\bar{M}_{yy}-\bar{M}_{yy}^{T}) \text{ or } \psi, \quad (M_{yy}-M_{yy}^{T}) \text{ or } w^{\circ}, \quad Q_{yy} \text{ or } w \tag{A3b}$$

where we have the following definitions for Q_{xx} and Q_{yy}:

$$Q_{xx} = (M_{xx}-M_{xx}^{T})'+(M_{xy}-M_{xy}^{T})^{\cdot}-(N_{xx}-N_{xx}^{T})w'-(N_{xy}-N_{xy}^{T})w^{\cdot}-P_2\ddot{u}-P_5\ddot{\phi}+P_4\ddot{w}',$$
$$Q_{yy} = (M_{yy}-M_{yy}^{T})^{\cdot}+(M_{xy}-M_{xx}^{T})'-(N_{xy}-N_{xy}^{T})w'-(N_{yy}-N_{yy}^{T})w^{\cdot}-P_2\ddot{v}-P_5\ddot{\psi}+P_4\ddot{w}^{\cdot}. \tag{A4}$$

APPENDIX B

Expressions for $a_1, a_2, \ldots, d_3$ appearing in (11)

$$\begin{bmatrix} A_{11}M^2+A_{66}N^2 & (A_{12}+A_{66})MN & 2\bar{B}_{16}MN & \bar{B}_{16}M^2+\bar{B}_{26}N^2 \\ & A_{66}M^2+A_{22}N^2 & \bar{B}_{16}M^2+\bar{B}_{26}N^2 & 2\bar{B}_{26}MN \\ \text{Symm.} & & \bar{D}_{11}M^2+\bar{D}_{66}N^2+\bar{A}_{44} & (\bar{D}_{12}+\bar{D}_{66})MN \\ & & & \bar{D}_{66}M^2+\bar{D}_{22}N^2+\bar{A}_{55} \end{bmatrix} \begin{bmatrix} a_1 \\ b_1 \\ c_1 \\ d_1 \end{bmatrix} = \begin{bmatrix} f_1 \\ f_2 \\ f_3 \\ f_4 \end{bmatrix},$$

$$\begin{bmatrix} A_{11}M^2+A_{66}N^2 & (A_{12}+A_{66})MN & 2\bar{B}_{16}MN & \bar{B}_{16}M^2+\bar{B}_{26}N^2 \\ & A_{66}M^2+A_{22}N^2 & \bar{B}_{16}M^2+\bar{B}_{26}N^2 & 2\bar{B}_{26}MN \\ \text{Symm.} & & \bar{D}_{11}M^2+\bar{D}_{66}N^2+\dfrac{\bar{A}_{44}}{4} & (\bar{D}_{12}+\bar{D}_{66})MN \\ & & & \bar{D}_{66}M^2+\bar{D}_{22}N^2+\dfrac{\bar{A}_{55}}{4} \end{bmatrix} \begin{bmatrix} a_3 \\ b_3 \\ c_3 \\ d_3 \end{bmatrix} = \begin{bmatrix} f_5 \\ f_6 \\ f_7 \\ f_8 \end{bmatrix},$$

$$\begin{bmatrix} A_{11} & \bar{B}_{16} & 0 & 0 \\ \bar{B}_{16} & \bar{D}_{66}+\dfrac{\bar{A}_{55}}{4M^2} & 0 & 0 \\ 0 & 0 & A_{22} & \bar{B}_{26} \\ 0 & 0 & \bar{B}_{26} & \bar{D}_{66}+\dfrac{\bar{A}_{44}}{4N^2} \end{bmatrix} \begin{bmatrix} a_2 \\ d_2 \\ b_2 \\ c_2 \end{bmatrix} = \begin{bmatrix} f_9 \\ f_{10} \\ f_{11} \\ f_{12} \end{bmatrix},$$

where f_1–f_{12} are given by

$$f_1 = 3B_{16}M^2N+B_{26}N^3, \quad f_2 = 3B_{26}MN^2+B_{16}M^3, \quad f_3 = \bar{D}_{11}M^3+(\bar{D}_{12}+2\bar{D}_{66})MN^2,$$
$$f_4 = \bar{D}_{22}N^3+(\bar{D}_{12}+2\bar{D}_{66})M^2N, \quad f_5 = \tfrac{1}{16}(A_{11}M^3+A_{12}MN^2+2A_{66}MN^2),$$
$$f_6 = \tfrac{1}{16}(A_{22}N^3+A_{12}NM^2+2A_{66}NM^2), \quad f_7 = \tfrac{1}{16}(3\bar{B}_{16}M^2N+\bar{B}_{26}N^3), \quad f_8 = \tfrac{1}{16}(3\bar{B}_{26}N^2M+\bar{B}_{16}M^3),$$
$$f_9 = \frac{1}{16M^2}(A_{12}N^2M-A_{11}M^3), \quad f_{10} = \frac{1}{16M^2}(\bar{B}_{26}N^2M-\bar{B}_{16}M^3),$$
$$f_{11} = \frac{1}{16N^2}(A_{12}M^2N-A_{22}N^3), \quad f_{12} = \frac{1}{16N^2}(\bar{B}_{16}M^2N-\bar{B}_{26}N^3).$$

Expressions for s_1–s_{23} are given as

$$s_1 = A_{11}a_1M+A_{12}b_1N-2B_{16}MN+\bar{B}_{16}(c_1N+d_1M), \quad s_2 = A_{11}(2a_2M+M^2/8)-A_{12}N^2/8+2\bar{B}_{16}d_2M,$$
$$s_3 = -A_{11}M^2/8+2A_{12}Nb_2+A_{12}N^2/8+2\bar{B}_{16}c_2N,$$
$$s_4 = 2A_{11}a_3M-A_{11}M^2/8+2A_{12}b_3N-A_{12}N^2/8+2\bar{B}_{16}(c_3N+d_3M),$$
$$s_5 = A_{11}M^2/8+A_{12}N^2/8, \quad s_6 = A_{12}a_1M+A_{22}b_1N-2B_{26}MN+\bar{B}_{26}(c_1N+d_1M),$$
$$s_7 = A_{12}(2a_2M+M^2/8)-A_{22}N^2/8+2\bar{B}_{26}d_2M, \quad s_8 = -A_{12}M^2/8+2A_{22}Nb_2+A_{22}N^2/8+2\bar{B}_{26}c_2N,$$
$$s_9 = 2A_{12}a_3M-A_{12}M^2/8+2A_{22}b_3N-A_{22}N^2/8+2\bar{B}_{26}(c_3N+d_3M),$$
$$s_{10} = A_{12}M^2/8+A_{22}N^2/8, \quad s_{11} = B_{16}M^2+B_{26}N^2-A_{66}a_1N-A_{66}b_1M-\bar{B}_{16}c_1M-\bar{B}_{26}d_1N,$$
$$s_{12} = A_{66}MN/4-2A_{66}a_3N-2A_{66}b_3M-2\bar{B}_{16}c_3M-2\bar{B}_{26}d_3N,$$
$$s_{13} = -D_{11}M^2-D_{12}N^2+B_{16}a_1N+B_{16}b_1M+\bar{D}_{11}c_1M+\bar{D}_{12}d_1N,$$
$$s_{14} = -B_{16}MN/4+2B_{16}a_3N+2B_{16}b_3M+2\bar{D}_{11}c_3M+2\bar{D}_{12}d_3N,$$
$$s_{15} = -D_{12}M^2-D_{22}N^2+B_{26}a_1N+B_{26}b_1M+\bar{D}_{12}c_1M+\bar{D}_{22}d_1N,$$

$$s_{16} = -B_{26}MN/4+2B_{26}a_3N+2B_{26}b_3M+2\bar{D}_{12}c_3M+2\bar{D}_{22}d_3N,$$

$$s_{17} = -B_{16}a_1M-B_{26}b_1N+2D_{66}MN-\bar{D}_{66}(c_1N+D_1M),$$

$$s_{18} = -B_{16}(2a_2M+M^2/8)+B_{26}N^2/8-2\bar{D}_{66}d_2M, \quad s_{19} = B_{16}M^2/8-2B_{26}Nb_2-B_{26}N^2/8-2\bar{D}_{66}c_2N,$$

$$s_{20} = -2B_{16}a_3M+B_{16}M^2/8-2B_{26}b_3N+B_{26}N^2/8-2\bar{D}_{66}(c_3N+d_3M),$$

$$s_{21} = -B_{16}M^2/8-B_{26}N^2/8, \quad s_{22} = -s_{13}M^2-s_{15}N^2+2s_{17}MN,$$

$$s_{23} = (s_2M^2-s_3M^2-s_4M^2/2+s_{12}MN/2+2s_5M^2-s_7N^2+s_8N^2-s_9N^2/2+2s_{10}N^2+s_{12}MN/2)/2.$$